photonics

MDPI

Review

Recent Advances in Coherent Optical Communications for Short-Reach: Phase Retrieval Methods

Abdullah S. Karar [1], Abdul Rahman El Falou [1], Julien Moussa H. Barakat [1] and Zeynep Nilhan Gürkan [1] and Kangping Zhong [2,*]

[1] College of Engineering and Technology, American University of the Middle East, Egaila 54200, Kuwait
[2] POET Technologies Inc., Shenzhen 518057, China
* Correspondence: zhongkangping1987@gmail.com

Abstract: Short-reach transmission systems traditionally utilize intensity modulation (IM) at the transmitter and direct detection (DD) at the receiver due to their cost-effectiveness, small footprint, and low power consumption. However, with the exponential increase in bandwidth demand, coherent optical communication systems have become necessary for long-haul distances, requiring application-specific integrated circuits (ASIC) and advanced digital signal processing (DSP) algorithms coupled with high-speed digital-to-analog and analog-to-digital converters to achieve Tbit/s speeds. As coherent technology matures, it will eventually become feasible for short-reach transmission. In this context, self-coherent systems have emerged as an intermediary solution, offering advantages over traditional IM/DD systems. While comprehensive review studies exist on self-coherent transceivers, they do not cover recent advances in phase retrieval methods for short-reach optical communications. This review article highlights recent developments in cost-effective self-coherent detection for short-reach systems through comparing the benefits of single sideband (SSB) transmission and Kramers-Kronig detection to carrier-assisted phase retrieval, the Gerchberg-Saxton (GS) algorithm, and the transport of intensity equation (TIE) method.

Keywords: coherent detection; short-reach optical interconnects; analog signal processing; direct detection; Kramers-Kronig; low-latency; optical fiber communications; realtime; single-sideband; Hilbert transform

Citation: Karar, A.S.; Falou, A.R.E.; Barakat, J.M.H.; Gürkan, Z.N.; Zhong, K. Recent Advances in Coherent Optical Communications for Short-Reach: Phase Retrieval Methods. *Photonics* **2023**, *10*, 308. https://doi.org/10.3390/photonics10030308

Received: 31 January 2023
Revised: 25 February 2023
Accepted: 9 March 2023
Published: 13 March 2023

1. Introduction

1.1. The Bandwidth Demand

The Internet is experiencing a tremendous annual growth rate of 30% per year, as reported by Cisco [1]. This growth is driven by various factors such as online commerce, mobile applications, video-on-demand, cloud computing, social media, educational networking, Internet of Things (IoT), edge computing, and freelance journalism. The backbone of this growth is optical fiber communications, which enables these services and has brought about significant economic, social, and political changes. Today, optical fiber communication networks are considered the backbone of the Internet and the gateway to the information age. They also play an integral role in global infrastructure connectivity, enabling quick, low-cost, and reliable communication between communities, economies, and countries. In particular, the relentless growth in mobile connectivity will bring over two thirds of the world population online. Mobile broadband service development is being shaped by consumer expectations. Innovative solutions are needed to address the anticipated increases in traffic (projected to grow by a factor of 10–100 times between 2020 and 2030 according to the ITU reports [2]), manage the growth in the number of devices and services, and meet the demands for improved affordability and user experience. It is anticipated that by the year 2025, there will be 50 billion Internet-connected gadgets. According to Cisco annual reports [1], more than 70 percent of the world's population will

be connected via mobile, there will be 5.7 billion mobile customers worldwide, up from the 5.1 billion (66 percent of the population) in 2018. The number of devices connected to IP networks will be more than three times the global population and machine-to-machine connections will account for nearly half the global connected devices and connections by 2023 [2]. The global mobile data traffic forecasted by ITU in Exa-bytes per month, from 2020 to 2030, are depicted in Figure 1. The share of machine-to-machine traffic is growing within global traffic, a telltale of an upcoming IoT revolution.

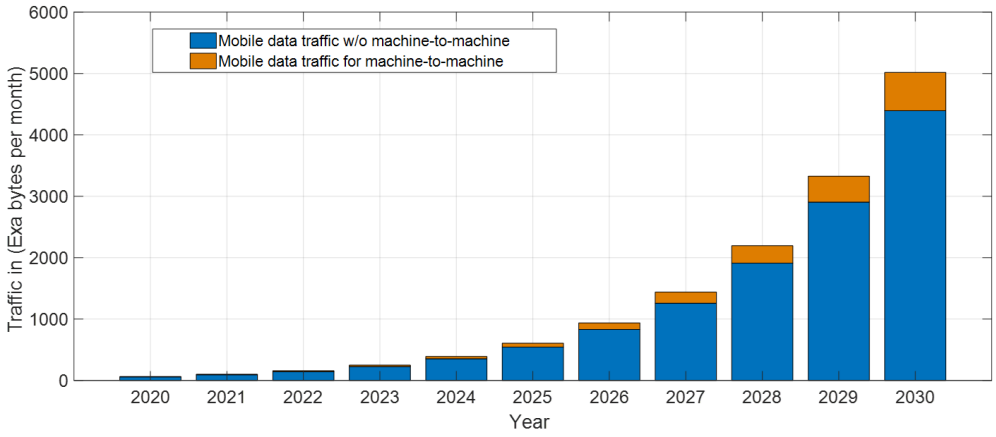

Figure 1. Global mobile data traffic forecast for the period 2020 to 2030 (ITU) [2].

5G, or fifth generation mobile technology, has enabled the expansion of innovative IoT solutions, edge computing, and cloud services, resulting in a surge of data flow in and out of data centers and access networks. This data flow aggregates into, the exponentially growing, global network traffic, which necessitates the processing, transmission [3], and storage of massive amounts of information in data centers, metro-links, and access networks. To meet this demand, scalable and cost-effective optical network infrastructures are required.

1.2. Connectivity in Short-Reach

Optical networks can be classified based on various factors such as reach, capacity (measured in bits per second), topology, and cost. Figure 2 illustrates different types of optical networks. Starting with data centers and carrier central offices, very short-reach (VSR) optical interconnects employ a point-to-point topology and have a distance of less than 1 km for standard single-mode fiber (SSMF) or less than 100 m for multi-mode fiber (MMF) as described in [4]. Access networks, which have a reach of less than 50 km, remain passive and support un-amplified transmission with large splitting factors, allowing for a broadcast topology, as noted in [5]. Metro networks typically have a ring topology and a transmission reach of less than 300 km, serving cities and metropolitan areas. An Erbium-Doped Fiber Amplifier (EDFA) is placed every 70–80 km of SSMF, as per [4]. Regional networks, deployed for inter-city communications, target a maximum reach of 600 km and employ a fully connected mesh topology. Lastly, long haul and sub-sea transmission links form the backbone of the entire network and are characterized by large transmission distances ranging from 600 km to 10,000 km.

In this article, short-reach optical communications is designed to enable transmission distances starting from 300 m to 100 km of SSMF, thus servicing applications in VSR, access and metropolitan area networks. This emerging market is further subdivided by length scale, as depicted in Figure 3. The short-reach (SR) intra data centers (DC) employ MMF at distances less than 300 m. Long range (LR) and extended range (ER) enable transmission over 20 km and 40 km of SSMF, respectively. Future plans are well underway to reach the limits of the unamplified transmission span of 80 km to 100 km. short-reach optical communications has emerged as the leading market segment, which must meet the bandwidth demand and distance requirements, while maintaining high throughput, low latency, small footprint and low power consumption at a low cost [6].

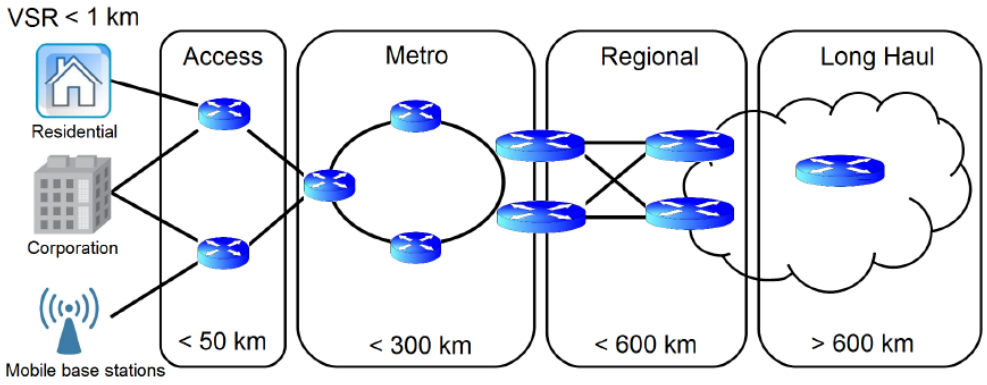

Figure 2. Examples of optical network topology and transmission reach, servicing data centers, access, metro, and long-haul links.

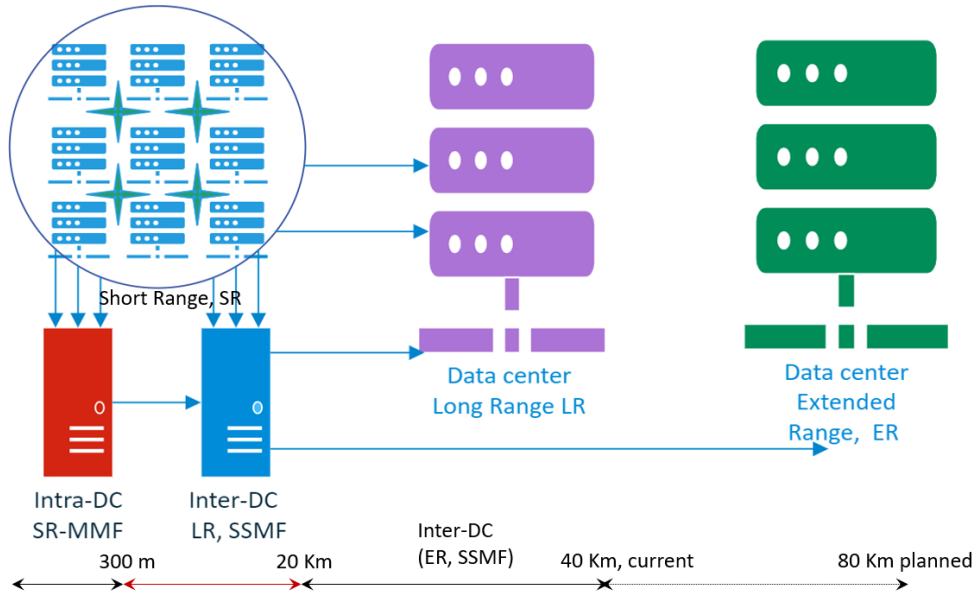

Figure 3. The length scales and potential applications of short-reach optical communications. SR: short-reach, MMF: multimode fiber, SSMF: standard single mode fiber, LR: long range, ER: extended range.

1.3. Bridging the Gap: Balancing Cost and Performance with Self-Coherent Technology

Due to the sheer number of deployable network elements, cost is a primary consideration in short-reach optical interconnects, in contrast to long-haul optical transmission systems, which operate at data rates well above 200 Gb/s and 400 Gb/s [7], even reaching 800 Gb/s [8], and employ expensive coherent detection. However, the deployment of coherent detection in short-reach optical links is expensive. A more viable and cost efficient solution would be to utilize intensity modulation and direct detection (IM/DD) [9]. Regardless of whether short-reach or long-haul optical communication systems are deployed, fiber chromatic dispersion (CD) and attenuation remain the two primary limiting factors for data rate and transmission reach. In this discussion, it is assumed that fiber nonlinearity is managed by reducing the launch power, at which point fiber attenuation becomes the main factor limiting transmission reach. To overcome fiber attenuation, signal amplification is enabled via Erbium doped fiber amplifier (EDFAs) deployed every 80 km along the fiber link. Even with effective dispersion compensation, the accumulated amplified spontaneous emission (ASE) noise becomes the main source of impairment in long-haul transmission. In contrast, short-reach optical transmissions operate within a single span, without an inline EDFA, and are thus fundamentally limited by fiber dispersion as opposed to ASE noise.

Fiber CD causes the transmitted optical pulses to spread out in time, overlap and interfere with each other producing intersymbol interference (ISI). The received electrical field is, by extension, an output of a linear time invariant system, which can be easily compensated for with access to the complex (real and imaginary) components of the electrical field. The process of full-field recovery is achieved through coherent detection. In fact, long-haul transceivers utilize coherent detection and/or dual-parallel Mach-Zehnder modulators (DP-MZM), to completely compensate liner effects, including CD, as both the real (in-phase) and imaginary (quadrature) components of the electric field are manipulated at the transmitter and/or recovered at the receiver. The process of digitally pre-compensating or post-compensating for CD is known as electronic dispersion compensation (EDC). Coherent detection coupled with digital pre- and post- EDC, fiber chromatic dispersion is no longer the barrier limiting transmission reach. However, this would come at the cost of digital coherent receivers employing with high speed digital-to-analog converters (DACs) and analog-to-digital converters (ADCs), coupled with advance digital signal processing (DSP) algorithms implemented on an application specific integrated circuit (ASIC). The same does not hold for direct detection, where a photodiode applies square-law operation $|.|^2$, recovering the light intensity without the optical phase, which is lost. Furthermore, direct detection converts a simple linear compensation task into a complicated nonlinear equalization problem, with the received signal suffering from both linear distortions and nonlinear distortions. The former manifests as strong spectral dips in the fiber frequency-domain transfer function known as frequency selective power fading [10–12], while the latter results from signal-to-signal beating interference (SSBI) [12] and photodiode current series expansion. To overcome these limitations without the need to recover both real and imaginary components of the electrical field, digital pre- and post- equalization is necessary. These systems used feed-forward equalizers (FFE) and decision feedback equalizers (DFE) delivering 112 Gbit/s for distances up-to 20 km of single-mode fiber SSMF with directly modulated lasers [13] and chirp-free MZM [14]. It is possible to effectively mitigate ISI caused by the linear power fading without actually eliminating the nulls in the frequency spectrum [11] through methods of pre-coding [12,15] or spectral slicing around the power fading dips [16]. In particular, transmitter-side Tomlinson-Harashima pre-coding (THP) [12,15,17], utilizes a feedback path to subtract the predicted ISI induced by previous symbols [11,12]. In effect, THP is a DFE moved to the transmitter side with a modulo operation replacing the decision device and eliminating the problem of error-propagation present in receiver-side DFE [12,15]. The main drawback of the THP is the need for an additional decoding step at the receiver. Furthermore, the filter coefficients needed for THP must be known at the transmitter in advance, and consequently are calculated by means of a training-based DFE at the receiver [17]. The compensation of the nonlinear SSBI has been attempted using Volterra nonlinear equalizers VNLE [13,18–22], neural networks [21] and maximum likelihood sequence estimator (MLSE) [23]. The complexity of these DSP-based solutions, limited reach and data-rate hinders their potential application in short-reach optical communications.

There is a notable disparity between expensive coherent technology and low-cost IM/DD solutions. This economic gap is primarily driven by the cost per bit, which is heavily influenced by the technology used and the type of impairment being compensated for. For example, coherent transceivers are able to overcome CD, but are limited by amplified ASE noise. On the other hand, low-cost IM/DD transceivers are limited by their ability to mitigate CD while still maintaining simplicity. To bridge this gap, a variety of self-coherent solutions have emerged beyond EDC with digital coherent transceivers, such as single sideband (SSB) modulation with Kramers-Kronig (KK) receivers. Recently, phase retrieval algorithms have also shown promise in short-reach transmission. The structure of the remainder of this paper is as follows: In Section 2, we provide a brief overview of EDC with coherent transmission and detection. Section 3 presents a comprehensive review of SSB modulation with the KK receiver. Section 4 delves into the recent advancements in the

use of iterative phase retrieval algorithms for pre- and post- CD compensation. Finally, a conclusion and future trends are presented in Section 6.

2. Electronic Dispersion Compensation

DSP in optical communication systems is enabled by high speed DAC and ADC technology operating at billions of samples per second. Fiber chromatic dispersion can be effectively mitigated through EDC at the transmitter and/or at the receiver. The former requires DSP of the drive signals to an external I/Q modulator, while the latter uses polarization diversity coherent detection with post DSP. A schematic diagram of a DSP enabled digital coherent transceiver is shown in Figure 4. At the transmitter, the incoming binary data through the client serializer/deserializer (SERDES) interface, have the option of probabilistic shaping (PS) by means of a distribution matcher prior to forward error correct (FEC) encoding. Probabilistic shaping (PS) is a method applied in digital communications to enhance the spectral efficiency and signa-to-noise ratio (SNR) by altering the probability distribution of the signal before it is encoded with FEC codes [8]. In most long-haul coherent systems, soft-decision (SD) low-density parity-check (LDPC) are used in FEC [24]. The encoded binary data are subsequently mapped into symbols, in a minimum of four dimensions, in-phase (I) and quadrature (Q) component of each of the two orthogonal states of polarization X and Y. Pilot insertion and spectral shaping is then possible on the symbol level with digital subcarrier multiplexing [8]. The symbols are up-sampled before CD pre-compensation using finite impulse response (FIR) filters [25]. Pre-emphasis for compensating the transmitter bandwidth limitations is performed before converting the digital signal into analog drive voltages using DACs. Trans-impedance amplifiers (TIA) are used to provide the adequate voltage swing to the external modulators. In long-haul coherent systems, externally modulated transmitters provide the capability to adjust the amplitude and phase of the complex optical field through a dual-parallel or dual-drive MZM configuration [26]. A dual-parallel MZM, also known as a Cartesian or I/Q modulator, is a nested MZM structure that grants full control over the optical field through two drive voltages. In contrast, a dual-drive MZM is a simpler device that only allows limited control over the complex optical field through a restricted access to the complex plan [27]. Lithium Niobate ($LiNbO_3$) external modulators are commonly used in long-haul transmission systems [28], but they are large, costly, and require intricate bias control circuits, making them less suitable for short-range applications.

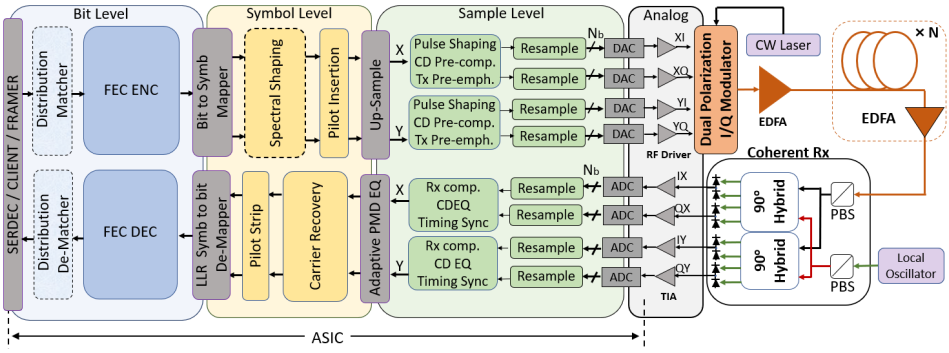

Figure 4. A schematic diagram of a DSP enabled digital coherent transceiver.

EDC schemes at the receiver-end are largely dependent on the receiver configuration. Coherent detection preserves both the amplitude and phase of the received complex optical field, allowing for linear compensation of dispersion electronically [29]. In these receivers a local oscillator (LO) is mixed with the incoming optical signal through a 90° optical hybrid producing photodetected currents for the I/Q components of the complex optical field [30]. Digital coherent transceivers utilize a linear mapping of signals between the optical and digital domains to compensate for channel impairments such as chromatic dispersion, and polarization mode dispersion (PMD), which have historically hindered

the data rate and transmission distance of direct detection systems. To invert the fiber transfer function and account for dispersion, a fixed FIR with a lot of taps is typically utilized [31]. Fast Fourier transform operations are used in the frequency domain chromatic dispersion equalization (CDEQ) strategy, which is better suited for compensating significant accumulated dispersion [29]. Then, for polarization demultiplexing, PMD mitigation, and residual dispersion [32], an adaptive equalizer is used. The frequency offset between the LO and received signal is reduced prior to carrier phase recovery using DSP methods that are specific to the chosen modulation format [29]. Coherent detection with DSP support, not only enables dispersion post-compensation, but also demodulates quadrature amplitude modulation (QAM) formats, ushering in an innovative new era of optical fiber communications with significant enhancements to system functionality and capacity [32].

The design of coherent transceivers is determined by the specific application they will be used for. For example, short-range transmission systems require low-power, low-complexity transceivers that are suitable for small form factor pluggable devices. However, the cost of digital coherent systems is still too high for widespread deployment in short-reach optical communications. Despite this, significant efforts have been made to optimize data rate and tailor the digital pre- and post-processing to match the unique specifications and impairments of each physical link. While digital coherent transceivers are considered the long-term solution for short-range optical communications, their current cost remains a barrier to widespread deployment.

3. Self-Coherent Transceivers

Coherent receivers, rely on mixing an LO with a randomly polarized and rotated received optical signal, which inherently require a polarization diversity set-up to linearly map the optical field into the electrical domain. The implementation of a polarization diversity setup, effectively doubles the number of detection components necessary for proper full-field recovery. In an effort to reduce costs, self-coherent systems eliminate the need for an LO at the receiver, by generating a reference CW carrier at the transmitter, which is sent alongside the signal. Various self-coherent detection schemes have been proposed, such as the Kramers-Kronig receiver [33], Stokes-vector receiver [34], carrier-assisted differential detection [35], and asymmetric self-coherent detection [36]. Regardless of the type of self-coherent detection employed, the advantages go beyond the ability to compensate CD. Specifically, these advantages include the following: (i) reduced DSP and ASIC complexity as no carrier recovery or frequency offset estimation is needed, (ii) reduced cost through eliminating the need for dual-polarization detection and receiver LO, and (iii) an additional degree of freedom becomes available increasing the spectral efficiency. A comprehensive and in-depth review of recent advancements in self-coherent transceivers can be found in [5]. Among the various techniques, single-sideband modulation (SSB) with the Kramers-Kronig (KK) receiver [33] appears to be the most promising candidate for implementation in short-reach optical communications. This approach utilizes a single single-ended photodetector and reconstructs the full single-polarization optical field through DSP [37]. Therefore, the SSB+KK approach is the primary focus of this article. Furthermore, the review in [5] was conducted before a recent surge in research on phase retrieval algorithms for double side-band (DSB) and SSB modulations. In light of these recent developments, the SSB+KK approach is compared to the carrier-assisted phase retrieval schemes [35,38] in this article.

3.1. Single-Side-Band Modulation

A DSB signal is composed of a right-side-band (RSB) and left-side-band (LSB). In principle, the RSB and LSB could be two distinct and independent complex-valued signals, named in the time domain as $s_R(t)$ and $s_L(t)$, respectively. In the case of the $s_R(t) = s_L^*(t)$, the DSB signal is real-valued and the spectrum is said to be conjugate symmetric. A signal with either an LSB only or RSB only is said to be SSB. Examples of four primary methods for generating an SSB signal is shown in Figure 5:

- Utilizing two DACs to create both the I and Q components of a complex-valued SSB signal, which is then modulated using a dual-drive MZM (DDMZM) [39], capable of complex modulation. The DDMZM is biased at the quadrature point to induce a DC carrier and is depicted in Figure 5a.
- Utilizing two DACs to create both the I and Q components of a complex-valued SSB signal, which is then modulated using a nest IQ modulator [40,41], also known as a dual-parallel MZM (DPMZM) with a digitally induced virtual carrier as depicted in Figure 5b.
- Using a single DAC to produce a real-valued DSB signal with a single drive MZM, followed by an optical bandpass filter (OBPF) to remove either LSB or RSB producing a quasi-SSB signal [42–44]. This is also known as vestigial side-band (VSB), as depicted in Figure 5c.
- Utilizing two DACs to create both the phase and amplitude of a complex-valued SSB signal, for the dual modulation of a directly modulated laser (DML) integrated with a electroabsorption modulator (EAM) [45], as depicted in Figure 5d. The former acts as a phase modulator with a strong chirp effect, while the latter acts as an intensity modulator [46].

The DDMZM and DPMZM approaches can produce a rigorous SSB, while the optical filtering approach produces a quasi-SSB due to the non-ideal OBPF, resulting in residual frequency content of the filtered side-band persisting. Recent studies [45] have shown that the optical IQ modulator generates the highest-quality signal but is complex, while the DDMZM is cost-effective but has limited dynamic range. The optical filtering approach in Figure 5c is easy to implement but has high requirements for no-guardband optical SSB signals, reducing spectral efficiency. Conventional schemes in Figure 5a–c suffer from complicated control, large insertion loss, and large footprint. However, EML-based schemes, similar to that of Figure 5d, exhibit lower cost and high output power, with the dual modulation of DML integrated with an EML having the simplest structure [45,46]. Practical issues include adding the optical carrier and implementing the Hilbert transform, which can be achieved in either digital or analog domains [46].

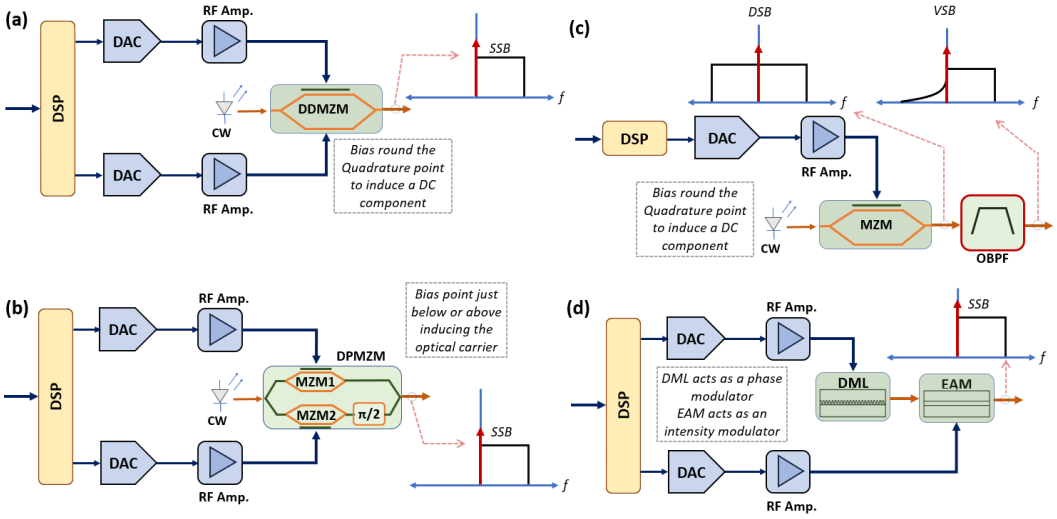

Figure 5. A representative depiction of four primary SSB signals generation techniques: (**a**) Dual drive MZM (DDMZM) biased at the quadrature point to induce a DC component, (**b**) Dual Parallel MZM (DPMZM) with virtually induced carrier, (**c**) Single drive MZM in tandem with an OBPF producing a vestigial side-band (VSB) signal, (**d**) Dual modulation of a DML integrated with an EAM.

3.2. Kramers-Kronig Receiver

The Kramers-Kronig relations are mathematical relations that allow one to calculate the real part from the imaginary part, or imaginary part from the real part, of an analytic complex function. These relations are named after physicists Ralph Kronig, who developed

a theory of X-ray absorption [47], and Hans Kramers, who worked on the interaction of electromagnetic waves with matter.

The use of KK relations in short-reach optical receivers was proposed in [33]. It has been demonstrated that the KK relations can be used to extract the phase information of an optical signal from the detected photocurrent, thereby allowing for full-field reconstruction at the receiver. KK-based receivers offer a promising solution for detecting the complex envelope of an SSB signal [48], using a single photo-diode and DSP to remove signal-to-signal beating interference [49,50]. This is made possible by the fact that, the complex envelope of an SSB signal is analytic, and the real and imaginary parts of this signal are related through a Hilbert transform [6]. This relation can be used to retrieve the phase of the received SSB signal from its magnitude, assuming the signal is minimum-phase [51]. Consequently, the reconstruction of the optical field using KK relations requires that the received optical signal maintain the minimum-phase condition, which is generally satisfied if the power of the optical carrier is large enough compared to the optical signal power. A signal is considered to be minimum-phase if its Z-transform is expressed by a rational function, and all poles and zeros are located inside the unit circle of the complex Z-plane. A necessary and sufficient condition for an SSB signal to be minimum-phase was given in [51], requiring that the trajectory of the received signal in the complex plane not encircle the origin. This condition can be met by a large enough carrier-to-sideband power ratio (CSPR). Ideally, a CSPR of 6 dB is sufficient to achieve this requirement. After retrieving the phase of the received SSB signal from its magnitude, EDC can be performed at the receiver. There are both optical [52–54], and electrical [33,48,50,55,56] means to meet minimum phase requirement.

The operation of the KK receiver is best illustrated using the embodiment in Figure 6. A low-cost transmitter producing a VSB signal for PAM4 signal is transmitted over one or more spans of SSMF. A single photo-diode is used at the receiver. Let us denote the optical carrier by $A_c e^{j\omega_c t}$, and the optical complex data signal by $s(t)e^{j\omega_s t}$; then the received optical signal prior-to the photo-diode input $E(t)$ can be written as [57]:

$$E(t) = (A_c + s(t)e^{j(\omega_s - \omega_c)t})e^{j\omega_c t} \tag{1}$$

The photodiode current $I(t)$ after photo detection is proportional to the power of the received electrical field in (1) through square-law detection. Without loss of generality and disregarding scaling factors, the equation of the current $I(t)$ can be expressed as:

$$\begin{aligned} I(t) = |E(t)|^2 &= (A_c + s(t)e^{j(\omega_s - \omega_c)t})^2 \\ &= A_c^2 + s(t)^2 + 2\Re\left\{(A_c \times s(t) \times e^{j(\omega_s - \omega_c)t}\right\} \end{aligned} \tag{2}$$

where $\Re(.)$ is the real part of the complex argument. The power spectrum of $I(t)$ has three primary contributions, originating from: the signal–signal beating $s(t)^2$, the carrier–carrier beating A_c^2, and the signal–carrier beating $2\Re(A_c \times s(t) \times e^{j(\omega_s - \omega_c)t})$. The photocurrent $I(t)$ is sampled and quantized by an ADC at the output of photodiode and then sent to DSP to fully extract the optical field using KK algorithm which is depicted in inset of Figure 6. The optical phase $\phi(t)$ can be estimated from the photodiode current $I(t)$ using the following expression:

$$\phi(t) = \mathcal{H}\left[\ln\left(\sqrt{I(t)}\right)\right] \tag{3}$$

where $\mathcal{H}[.]$ denotes the Hilbert transform of the argument. Thus, the optical complex data signal $s(t)$ can be recovered and expressed as [5]:

$$s(t) = [\sqrt{I(t)}e^{j\phi(t)} - A_c]e^{-j(\omega_s - \omega_c)t} \tag{4}$$

Additionally, the process can include digital downsampling, and subsequently various DSP techniques such as electrical equalization, carrier recovery and demodulation can be

applied. Table 1 presents a compilation of the latest transmission demonstrations that have broken records in terms of data-rate and distance product, utilizing SSB modulation and a KK receiver.

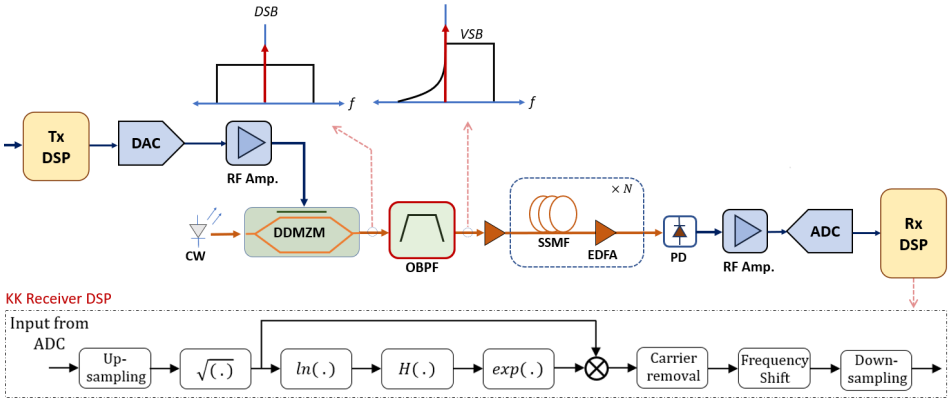

Figure 6. KK algorithm implemented in DSP for full optical field reconstruction.

Table 1. Recent demonstrations that have broken records in terms of data-rate and transmission distance with SSB modulation and KK receiver.

Distance (km)	Data-Rate (Gbps)	Modulation	CSPR (dB)	Optimum Launch Power (dBm)	Comments	Ref.
100	220	32-QAM	9	2	Single diode, Single channel, Single polarization	[37]
240	112	16-QAM	11	2.5	WDM DD SSB, Nyquist-SCM	[58]
300	267	16-QAM	-	-	-	[57]
80	112	OFDM 16-QAM	10	7	-	[59]
80	168	64-QAM	12	2	WDM	[60]
960	112	4-PAM	12	5	WDM	[61]
160	80	OFDM	8	-	-	[62]
80	224	4-PAM	-	-	VC-SSB	[63]
80	120	16-QAM	12	10	w/o amplification, w/NN NLE	[64]
80	400	64-QAM	14–16	8–9	SSB DD	[65]
320	200	4-PAM	11	4	SSB-LN-LSTM, WDM (32 channels)	[66]

4. Phase Retrieval Algorithms

Phase retrieval is a broad field that encompasses techniques used to solve the phase problem, which refers to determining the phase of a complex signal from measurements of its Fourier amplitude or intensity only [67]. In addition to the Kramers-Kronig relations, other popular methods for phase retrieval include the Gerchberg-Saxton (GS) algorithm [68] and the transport of intensity equation (TIE) method [69]. These techniques have found application in various fields including optical communications.

4.1. Transport of Intensity Equation (TIE)

The temporal transport of intensity equation (TIE) is a mathematical relationship that connects changes in the phase of a signal over time to variations in the power profile of the signal as it propagates through a dispersive medium [69]. By measuring the power

profile of a signal before and after it has passed through a short section of dispersive material, and using this information to solve the temporal TIE, it is possible to reconstruct the phase profile of the original signal [70]. This approach to phase reconstruction is known as temporal TIE. The utilization of the TIE for phase retrieval has been introduced in the context of optical pulse shaping on pico- femto- second time scales [70,71]. A representative example of using the TIE method for full-field reconstruction is shown in Figure 7. The DSP provides a non-iterative solution for phase reconstruction based on solving [69]:

$$\frac{\partial}{\partial t}\left(P\frac{\partial \phi}{\partial t}\right) = \frac{1}{\beta_2}\frac{\partial P}{\partial z} \tag{5}$$

where the power profile of the signal is denoted $P(t,z)$, while the phase of the signal is denoted $\phi(t,z)$. The schematic showing an example for a TIE based coherent receiver is shown in Figure 7 [69].

4.2. Gerchberg-Saxton (GS) Algorithm

One of the most widely used methods for phase retrieval is the Gerchberg-Saxton (GS) algorithm [68], which is an iterative method that alternates between the Fourier and spatial domains. The algorithm starts with an initial guess of the signal or image and iteratively updates it based on the constraint that the magnitude of the measured data is preserved. The GS algorithm and its variations are widely used in various fields such as optics, microscopy, X-ray diffraction, and quantum information. The application of the GS algorithm to short-reach optical communications primarily focuses on transmitter pre-EDC or receiver post-EDC.

The GS algorithm was demonstrated for pre-EDC in IM/DD transmission in both theoretical [72] and experimental [73,74] settings. The iterative GS algorithm fundamentally linearizes the IM/DD channel effect including square-law detection through treating the optical phase after direct detection as degree of freedom, while optimizing the optical amplitude at the transmitter to compensate for both CD induced power fading and nonlinear distortion. The GS algorithm was modified to reduce the implementation complexity and speed up convergence in [75–77], implemented at the receiver as a data-aided decision directed equalizer in [78], while a multi-constraint and error-controlled version of the GS algorithm was experimentally reported in [79], and [80], respectively. Recently, the iterative GS algorithm was used in designing a finite impulse response filter (FIR) at the transmitter for mitigating power fading ISI. The theoretical details of the GS-FIR filter are reported in [10], while the first experimental demonstration of such a filter is reported in [81].

4.2.1. Carrier-Less GS Phase Retrieval

The GS algorithm has enabled phase-retrieval (PR) receivers that reconstruct complex-valued signals using direct detection without optical carriers [82–84]. This is achieved through employing two photodiodes and a dispersive element and searching for the optimum phase that satisfies the relationship between the alternating projections. Two PR receiver solutions are proposed in [82] and demonstrated with faster convergence and high retrieved phase accuracy. The first solution involves a modified Gerchberg-Saxton algorithm that uses parallel alternative projections as intensity constraints. The second solution employs an enhanced single projection GS algorithm with selective phase reset using symbol-wise GS errors. The proposed solutions are tested by reconstructing a 30 Gbaud QPSK signal after 55 km single-mode fiber transmission. In [83], the authors demonstrate full-field detection of carrier-less polarization-multiplexed signals using direct-detection/intensity only measurements and phase-retrieval techniques based on dispersive element. An adaptive intensity transformation-based phase retrieval with high accuracy and fast convergence was proposed in [84]. In comparison to recently reported PR receivers, the proposed PR receiver in [84] reduces the required optical signal-to-noise ratio by 1.95 and 1.89 dB. The key advantage of the aforementioned GS-based approaches is eliminating

the need for the optical carrier. However, this comes at the cost of a large number of iterations and reliance on pilot symbols with large overhead.

4.2.2. Carrier-Assisted GS Phase Retrieval

In an effort to overcome the high complexity of the carrier-less GS schemes, the carrier at 0 GHz can be re-introduced to reduce the phase ambiguity in the GS algorithm. To that end, a carrier-assisted phase retrieval (CA-PR) algorithm was proposed for short-reach optical communications [38] based the iterative GS algorithm supporting both centered (CCA-PR) and edge (ECA-PR) carrier locations. The schematic showing a representative example for the GS-based carrier-assisted coherent receiver is shown in Figure 7. In fact, both TIE [69] and GS-based phase retrieval schemes exhibit nearly identical set-ups; thus, the two schemes demand similar hardware complexity [38].

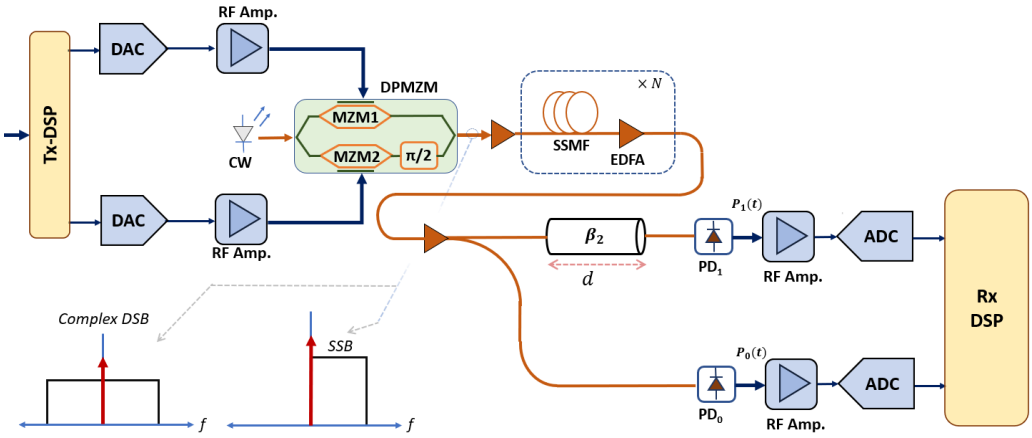

Figure 7. The simplest schematic showing carrier-assisted phase retrieval with TIE or GS approaches.

5. Carrier-Assisted Differential Detection

Carrier-assisted differential detection (CADD) is a direct detection method utilized in optical communications for retrieving the complex-valued optical field of a double sideband (DSB) signal, without resorting to coherent detection [35]. The CADD receiver utilizes a carrier signal that is added to the received signal, generating a so called difference signal that is then amplified and detected by a photodiode. Through processing the difference signal, the receiver can retrieve the original optical field of the DSB signal. CADD offers higher spectral efficiency and lower receiver complexity in comparison to other direct detection techniques, making it an attractive solution for short-distance optical communication applications such as data center interconnects [85].

Recently, a simplified symmetric carrier-assisted differential detection (S-CADD) receiver structure was proposed to compensate for SSBI impairment [86]. A low-complexity iterative SSBI mitigation algorithm was also proposed. The study in [86] compares the OSNR sensitivity, BER performance, and received optical power sensitivity for both S-CADD and asymmetric CADD (A-CADD) receivers.

Table 2, presents a comparison of the complexity of different phase retrieval schemes, including the self-coherent scheme and the TIE scheme, in reference to single polarization full coherent detection. The data was adopted from [38] and has been extended for this study.

Table 2. A comparison of different phase retrieval schemes: KK, ECA-PR, CCA-PR and TIE in reference to single polarization (SP) full coherent. BPD: balanced photodetector, SPD: single-ended photodetector, ODL: optical delay line, B: signal bandwidth, G: guard band, and F: frequency offset.

Scheme	Tx BW (GHz)	Key Optical Devices	# of ADC	# of PD	Rx BW (GHz)	OSNR Penalty (dB)	CSPR (dB)	Ref.
SP - Full Coherent	B/2	Optical hybrid	2	2 BPDs	B/2+F	-	-	-
KK	B/2	-	1	SPD	B	7.3	6	[33]
SVR	B/2	Optical Hybrid, 2 Couplers (1 × 2), PBS	3	3 BPDs	B/2	6	0	[34]
SVR	B/2	2 Couplers (1 × 2, 3 × 3), PBS	4	4 BPDs	B/2	6	0	[87]
STD-PR	B/2	2 Couplers (1 × 4, 3 × 3), Dispersive Element, 2 ODLs	4	4 BPDs	B	2	-	[88]
CADD	B/2+G	Optical Hybrid, 2 Couplers (1 × 2), ODL	3	2 BPDs, SPD	B/2+G	14	10	[35]
ECA-PR	B/2	Dispersive			B	3.8	−1	[38]
CCA-PR	B/2 + G	Element +	2	2 SPDs	B	5.5	1	[38]
TIE	B/2 + G	Coupler (1 × 2)			>B	10.3	11	[69]

6. Conclusions and Future Trends

Short-reach transmission systems traditionally employed IM/DD, due to their low cost, small foot-print and low power consumption. However, with the exponential growth in bandwidth demand, it became necessary to employ DSP-empowered, ASIC-enabled coherent digital transceivers for long-haul transmission. An emerging market gap exists between expensive coherent technology, which is limited by ASE noise, as opposed to dispersion limited cost-effective self-coherent solutions. Recent advances in cost-effective coherent detection in short-reach systems were highlighted. The Kramers-Kronig receiver coupled with single side-band modulation, was found to be the most promising candidate for short- to medium-reach access networks. Recent progress in carrier-assisted phase retrieval algorithms based on the transport of intensity equation and those based on the Gercbburg-Saxston iterative algorithm are introduced and compared to the KK schemes. Each of the schemes have their own set of advantages and disadvantages. An additional flexibility can be expected from the phase retrieval algorithms as they allow both edge- and carrier-centered solutions.

Author Contributions: Conceptualization, K.Z.; methodology, A.S.K., A.R.E.F. and K.Z.; software, A.S.K. and J.M.H.B.; investigation, Z.N.G. and J.M.H.B.; resources, J.M.H.B. and A.S.K.; writing—original draft preparation, A.S.K., A.R.E.F., K.Z. and Z.N.G.; writing—review and editing, K.Z. and Z.N.G.; supervision K.Z. All authors have read and agreed to the published version of the manuscript.

Funding: This research received no external funding.

Institutional Review Board Statement: Not applicable.

Informed Consent Statement: Not applicable.

Data Availability Statement: No new data were created or analyzed in this study. Data sharing is not applicable to this article.

Conflicts of Interest: The authors declare no conflict of interest.

References

1. *Cisco Annual Internet Report (2018–2023)*; White Paper; Cisco Systems: San Jose, CA, USA, 2022.
2. Union, I. IMT Traffic Estimates for the Years 2020 to 2030. *Rep. ITU* **2015**, *2370*. Available online: https://www.itu.int/pub/R-REP-M.2370 (accessed on 20 January 2023).
3. Banafaa, M.; Shayea, I.; Din, J.; Hadri Azmi, M.; Alashbi, A.; Ibrahim Daradkeh, Y.; Alhammadi, A. 6G Mobile Communication Technology: Requirements, Targets, Applications, Challenges, Advantages, and Opportunities. *Alex. Eng. J.* **2023**, *64*, 245–274. [CrossRef]
4. Cole, C. Beyond 100G client optics. *IEEE Commun. Mag.* **2012**, *50*, s58–s66. [CrossRef]
5. Alimi, I.; Patel, R.; Silva, N.; Sun, C.; Ji, H.; Shieh, W.; Pinto, A.; Muga, N. A Review of Self-Coherent Optical Transceivers: Fundamental Issues, Recent Advances, and Research Directions. *Appl. Sci.* **2021**, *11*, 7554. [CrossRef]

6. Chagnon, M. Optical Communications for short-reach. *J. Light. Technol.* **2019**, *37*, 1779–1797. [CrossRef]
7. IEEE P802.3bs 200 Gb/s and 400 Gb/s Ethernet Task Force. Available online:www.ieee802.org/3/bs/ (accessed on 20 July 2019).
8. Sun, H.; Torbatian, M.; Karimi, M.; Maher, R.; Thomson, S.; Tehrani, M.; Gao, Y.; Kumpera, A.; Soliman, G.; Kakkar, A.; et al. 800G DSP ASIC Design Using Probabilistic Shaping and Digital Sub-Carrier Multiplexing. *J. Light. Technol.* **2020**, *38*, 4744–4756. [CrossRef]
9. Pang, X.; Ozolins, O.; Gaiarin, S.; Olmedo, M.I.; Schatz, R.; Westergren, U.; Zibar, D.; Popov, S.; Jacobsen, G. Evaluation of High-Speed EML-based IM/DD links with PAM Modulations and Low-Complexity Equalization. In Proceedings of the ECOC 2016, 42nd European Conference on Optical Communication, Dusseldorf, Germany, 18–22 September, 2016; pp. 1–3.
10. Karar, A.S. Gerchberg-Saxton Based FIR Filter for Electronic Dispersion Compensation in IM/DD Transmission Part I: Theory and Simulation. *J. Light. Technol.* **2022**, *41*, 1335–1345 . [CrossRef]
11. Xin, H.; Zhang, K.; Kong, D.; Zhuge, Q.; Fu, Y.; Jia, S.; Hu, W.; Hu, H. Nonlinear Tomlinson-Harashima precoding for direct-detected double sideband PAM-4 transmission without dispersion compensation. *Opt. Express* **2019**, *27*, 19156–19167. [CrossRef]
12. Rath, R.; Clausen, D.; Ohlendorf, S.; Pachnicke, S.; Rosenkranz, W. Tomlinson–Harashima Precoding For Dispersion Uncompensated PAM-4 Transmission With Direct-Detection. *J. Light. Technol.* **2017**, *35*, 3909–3917. [CrossRef]
13. Gao, Y.; Cartledge, J.C.; Kashi, A.S.; Yam, S.S.H.; Matsui, Y. 112 Gb/s Single-Carrier PAM-4 Using a Directly Modulated Laser. In *Proceedings of the Advanced Photonics 2016 (IPR, NOMA, Sensors, Networks, SPPCom, SOF)*; Optica Publishing Group: Washington, DC, USA, 2016; p. SpM2E.2. [CrossRef]
14. Tang, X.; Qiao, Y.; Chen, Y.W.; Lu, Y.; Chang, G.K. Digital Pre- and Post-Equalization for C-Band 112-Gb/s PAM4 Short-Reach Transport Systems. *J. Light. Technol.* **2020**, *38*, 4683–4690. [CrossRef]
15. Wettlin, T.; Ohlendorf, S.; Rahman, T.; Wei, J.; Calabrò, S.; Stojanovic, N.; Pachnicke, S. Beyond 200 Gb/s PAM4 transmission using Tomlinson-Harashima precoding. In Proceedings of the 45th European Conference on Optical Communication (ECOC 2019), Dublin, Ireland, 22–26 September 2019; pp. 1–4. . [CrossRef]
16. Ros, F.D.; Ranzini, S.M.; Dischler, R.; Cem, A.; Aref, V.; Bülow, H.; Zibar, D. Machine-learning-based equalization for short-reach transmission: neural networks and reservoir computing. In *Proceedings of the Metro and Data Center Optical Networks and Short-Reach Links IV*; International Society for Optics and Photonics; Srivastava, A.K., Glick, M., Akasaka, Y., Eds.; SPIE: Bellingham, WA, USA, 2021; Volume 11712, pp. 1–8. [CrossRef]
17. Xiang, M.; Xing, Z.; El-Fiky, E.; Morsy-Osman, M.; Zhuge, Q.; Plant, D.V. Single-Lane 145 Gbit/s IM/DD Transmission With Faster-Than-Nyquist PAM4 Signaling. *IEEE Photonics Technol. Lett.* **2018**, *30*, 1238–1241. [CrossRef]
18. Yu, Y.; Choi, M.R.; Bo, T.; He, Z.; Che, Y.; Kim, H. Low-Complexity Second-Order Volterra Equalizer for DML-Based IM/DD Transmission System. *J. Light. Technol.* **2020**, *38*, 1735–1746. [CrossRef]
19. Stojanovic, N.; Karinou, F.; Qiang, Z.; Prodaniuc, C. Volterra and Wiener Equalizers for Short-Reach 100G PAM-4 Applications. *J. Light. Technol.* **2017**, *35*, 4583–4594. [CrossRef]
20. Diamantopoulos, N.P.; Nishi, H.; Kobayashi, W.; Takeda, K.; Kakitsuka, T.; Matsuo, S. On the Complexity Reduction of the Second-Order Volterra Nonlinear Equalizer for IM/DD Systems. *J. Light. Technol.* **2019**, *37*, 1214–1224. [CrossRef]
21. Zhang, W.; Ge, L.; Zhang, Y.; Liang, C.; He, Z. Compressed Nonlinear Equalizers for 112-Gbps Optical Interconnects: Efficiency and Stability. *Sensors* **2020**, *20*, 4680. [CrossRef]
22. Reza, A.G.; Troncoso-Costas, M.; Browning, C.; Diaz-Otero, F.J.; Barry, L.P. Single-Lane 54-Gbit/s PAM-4/8 Signal Transmissions Using 10G-Class Directly Modulated Lasers Enabled by Low-Complexity Nonlinear Digital Equalization. *IEEE Photonics J.* **2022**, *14*, 1–9. [CrossRef]
23. Randel, S.; Chandrasekhar, S.; Liu, X. Maximum likelihood sequence estimation for short-reach optical communications. *Opt. Express* **2008**, *16*, 8714–8722.
24. Tychopoulos, A.; Koufopavlou, O.; Tomkos, I. FEC in optical communications - A tutorial overview on the evolution of architectures and the future prospects of outband and inband FEC for optical communications. *IEEE Circuits Devices Mag.* **2006**, *22*, 79–86. [CrossRef]
25. Chen, R.; Zhang, W.; Li, S.; Gu, M. FIR filter-based electronic dispersion compensation for coherent optical systems. *Opt. Express* **2017**, *25*, 13584–13590.
26. Zhang, W.; Chen, R.; Li, D.; Li, S.; Gu, M. Dual-parallel Mach-Zehnder modulator with high extinction ratio and low drive voltage. *Opt. Express* **2007**, *15*, 3240–3244.
27. Wang, X.; Chen, R.; Li, S.; Gu, M. Dual-drive Mach-Zehnder modulator with improved linearity and reduced drive voltage. *Opt. Express* **2015**, *23*, 31107–31114.
28. Betts, G.; Cartledge, J. Overview of optical modulators and the properties that affect transmission system performance. In *Broadband Optical Modulators: Science, Technology, and Applications*; Chen, A.; Murphy, E., Eds.; CRC Press: Boca Raton, FL, USA, 2011; Chapter 4, pp. 93–126.
29. Savory, S.J.; Gavioli, G.; Killey, R.I.; Bayvel, P. Electronic compensation of chromatic dispersion using a digital coherent receiver. *Opt. Express* **2007**, *15*, 2120–2126. [CrossRef] [PubMed]
30. Sheikh, A.; Fougstedt, C.; Amat, A.G.i.; Johannisson, P.; Larsson-Edefors, P.; Karlsson, M. Dispersion Compensation FIR Filter With Improved Robustness to Coefficient Quantization Errors. *J. Light. Technol.* **2016**, *34*, 5110–5117. [CrossRef]
31. Jannson, T. Real-time Fourier transformation in dispersive optical fibers. *Opt. Lett.* **1983**, *8*, 232–234. [CrossRef]
32. Savory, S.J. Digital filters for coherent optical receivers. *Opt. Express* **2008**, *16*, 804–817. [CrossRef]
33. Mecozzi, A.; Antonelli, C.; Shtaif, M. Kramers–Kronig coherent receiver. *Optica* **2016**, *3*, 1220–1227. [CrossRef]

34. Che, D.; Li, A.; Chen, X.; Hu, Q.; Wang, Y.; Shieh, W. Stokes vector direct detection for linear complex optical channels. *J. Light. Technol.* **2015**, *33*, 678–684. [CrossRef]
35. Shieh, W.; Sun, C.; Ji, H. Carrier-assisted differential detection. *Light Sci. Appl.* **2020**, *9*, 18. [CrossRef]
36. Li, X.; O'Sullivan, M.; Xing, Z.; Alam, M.; Mousa-Pasandi, M.E.; Plant, D.V. Asymmetric self-coherent detection. *Opt. Exp.* **2021**, *29*, 25412–25427. [CrossRef]
37. Chen, X.; Antonelli, C.; Chandrasekhar, S.; Raybon, G.; Mecozzi, A.; Shtaif, M.; Winzer, P. Kramers–Kronig Receivers for 100-km Datacenter Interconnects. *J. Light. Technol.* **2018**, *36*, 79–89. [CrossRef]
38. Wu, Q.; Zhu, Y.; Hu, W. Carrier-Assisted Phase Retrieval. *J. Light. Technol.* **2022**, *40*, 5583–5596. [CrossRef]
39. Wang, X.; Liu, X.; Zhang, X.; Ong, C. Single-Sideband Generation Using a Dual-Drive Mach-Zehnder Modulator with a Phase-Locked Loop. *IEEE Photonics Technol. Lett.* **2008**, *20*, 268–270.
40. Wang, X.; Liu, X.; Zhang, X. Generation of Single-Sideband Signals Using an IQ Modulator and a Phase-Locked Loop. *IEEE Photonics Technol. Lett.* **2007**, *19*, 787–789.
41. Liu, X.; Wang, X.; Zhang, X.; Ong, C. A Stable Single-Sideband Generation Method Using an IQ Modulator and a Phase-Locked Loop. *IEEE Photonics Technol. Lett.* **2008**, *20*, 914–916.
42. Liu, X.; Wang, X.; Zhang, X. Generation of Quasi-Single-Sideband Signals Using a Single-Drive Mach-Zehnder Modulator and an Optical Filter. *Chin. Phys. Lett.* **2007**, *24*, 3143–3145.
43. Wang, X.; Liu, X.; Zhang, X. Quasi-Single-Sideband Generation Using a Single-Drive Mach-Zehnder Modulator and a Bandpass Filter. *IEEE Photonics Technol. Lett.* **2007**, *19*, 1–3.
44. Wang, X.; Liu, X.; Zhang, X. Single-Sideband Generation Using a Single-Drive Mach-Zehnder Modulator and a Bandpass Filter. *IEEE Photonics Technol. Lett.* **2006**, *18*, 2457–2459.
45. Bo, T.; Kim, H.; Tan, Z.; Dong, Y. Optical Single-Sideband Transmitters. *J. Light. Technol.* **2023**, *41*, 1163–1174. [CrossRef]
46. Kim, H. EML-Based Optical Single Sideband Transmitter. *IEEE Photonics Technol. Lett.* **2008**, *20*, 243–245. [CrossRef]
47. De Laer Kronig, R. On the Theory of Dispersion of X-rays. *J. Opt. Soc. Am.* **1926**, *12*, 547–557. [CrossRef]
48. Mecozzi, Andrea and Antonelli, Carlo and Shtaif, Maxim. Kramers-Kronig receivers. *Adv. Opt. Photonics* **2019**, *11*, 480–517. [CrossRef]
49. Chen, X.; Chandrasekhar, S.; Winzer, P. Self-Coherent Systems for short-reach Transmission. In Proceedings of the 2018 European Conference on Optical Communication (ECOC), Rome, Italy, 23–27 September 2018; pp. 1–3. [CrossRef]
50. Antonelli, C.; Mecozzi, A.; Shtaif, M. Kramers-Kronig PAM transceiver and twosided polarization-multiplexed Kramers-Kronig transceiver. *J. Light. Technol.* **2018**, *36*, 468–475. [CrossRef]
51. Mecozzi, A. A necessary and sufficient condition for minimum phase and implications for phase retrieval. *arXiv* **2016**, arXiv:1606.04861.
52. Schuh, K.; Le, S.T. 180 Gb/s 64QAM transmission over 480 km using a DFB laser and a Kramers-Kronig receiver. In Proceedings of the European Conference on Optical Communication, Rome, Italy, 23–27 September 2018; p. P.4.12.
53. Presi, M.; Cossu, G.; Contestabile, G.; Ciaramella, E.; Mecozzi, A.; Shraif, M. Transmission in 125-km SMF with 3.9 bit/s/Hz spectral efficiency using a single-drive MZM and a direct-detection Kramers-Kronig receiver without optical CD compensation. In Proceedings of the Optical Fiber Communication Conference, San Diego, CA, USA, 11–15 March 2018; p. Tu2D.3.
54. Zhu, M.; Zhang, J.; Ying, H.; Li, X.; Luo, M.; Huang, X.; Song, Y.; Li, F.; Yi, X.; Qiu, K. 56-Gb/s optical SSB PAM-4 transmission over 800-km SSMF using DDMZM transmitter and simplified direct detection Kramers-Kronig receiver. In Proceedings of the Optical Fiber Communication Conference, San Diego, CA, USA, 11–15 March 2018; p. M2C.5.
55. Randel, S.; Pilori, D.; Chandrasekhar, S.; Raybon, G.; Winzer, P. 100-Gb/s discrete-multitone transmission over 80-km SSMF using single-sideband modulation with novel interference-cancellation scheme. In Proceedings of the European Conference on Optical Communication, Valencia, Spain, 27 September–1 October 2015; p. 697.
56. Voelcker, H. Demodulation of single-sideband signals via envelope detection. *IEEE Trans. Commun. Technol.* **1966**, *14*, 22–30. [CrossRef]
57. Füllner, C.; Adib, M.M.H.; Wolf, S.; Kemal, J.N.; Freude, W.; Koos, C.; Randel, S. Complexity Analysis of the Kramers–Kronig Receiver. *J. Light. Technol.* **2019**, *37*, 4295–4307. [CrossRef]
58. Li, Z.; Sezer Erkılınç, M.; Shi, K.; Sillekens, E.; Galdino, L.; Xu, T.; Thomsen, B.C.; Bayvel, P.; Killey, R.I. Digital Linearization of Direct-Detection Transceivers for Spectrally Efficient 100 Gb/s/λ WDM Metro Networking. *J. Light. Technol.* **2018**, *36*, 27–36. [CrossRef]
59. Bo, T.; Kim, H. Kramers-Kronig receiver operable without digital upsampling. *Opt. Express* **2018**, *26*, 13810–13818. [CrossRef]
60. Li, Z.; Erkilinç, M.S.; Shi, K.; Sillekens, E.; Galdino, L.; Xu, T.; Thomsen, B.C.; Bayvel, P.; Killey, R.I. Spectrally Efficient 168 Gb/s/λ WDM 64-QAM Single-Sideband Nyquist-Subcarrier Modulation With Kramers–Kronig Direct-Detection Receivers. *J. Lightwave Technol.* **2018**, *36*, 1340–1346. [CrossRef]
61. Shu, L.; Li, J.; Wan, Z.; Yu, Z.; Li, X.; Luo, M.; Fu, S.; Xu, K. Single-photodiode 112-Gbit/s 16-QAM transmission over 960-km SSMF enabled by Kramers-Kronig detection and sparse I/Q Volterra filter. *Opt. Express* **2018**, *26*, 24564–24576. [CrossRef]
62. Sun, C.; Che, D.; Ji, H.; Shieh, W. Study of Chromatic Dispersion Impacts on Kramers–Kronig and SSBI Iterative Cancellation Receiver. *IEEE Photonics Technol. Lett.* **2019**, *31*, 303–306. [CrossRef]
63. Li, A.; Peng, W.R.; Cui, Y.; Bai, Y. 112GBd Virtual-carrier-assisted Single-Sideband PAM4 with Kramers-Kronig Detection and Blind Adaptive IQ Imbalance Compensation. In Proceedings of the Optical Fiber Communication Conference (OFC) 2019, San Diego, CA, USA, 3–7 March 2019; p. M1H.5. [CrossRef]

64. Chen, Z.; Wang, W.; Zou, D.; Ni, W.; Luo, D.; Li, F. Real-Valued Neural Network Nonlinear Equalization for Long-Reach PONs Based on SSB Modulation. *IEEE Photonics Technol. Lett.* **2023**, *35*, 167–170. [CrossRef]
65. Le, S.T.; Schuh, K.; Dischler, R.; Buchali, F.; Schmalen, L.; Buelow, H. Beyond 400 Gb/s Direct Detection Over 80 km for Data Center Interconnect Applications. *J. Light. Technol.* **2020**, *38*, 538–545. [CrossRef]
66. Fang, X.; Chen, X.; Yang, F.; Zhang, L.; Zhang, F. 6.4Tb/s SSB WDM Transmission Over 320km SSMF With Linear Network-Assisted LSTM. *IEEE Photonics Technol. Lett.* **2021**, *33*, 1407–1410. [CrossRef]
67. Nugent, K.; Paganin, D.; Gureyev, T. A phase odyssey. *Phys. Today* **2001**, *54*, 27–32. [CrossRef]
68. Gerchberg, R.; Saxton, W. A practical algorithm for the determination of phase from image and diffraction plane pictures. *Optik* **1972**, *35*, 237–246.
69. Matsumoto, M. Optical Signal Phase Reconstruction Based on Temporal Transport-of-Intensity Equation. *J. Light. Technol.* **2020**, *38*, 4722–4729. [CrossRef]
70. Cuadrado-Laborde, C.; Carrascosa, A.; Pérez-Millán, P.; Díez, A.; Cruz, J.; Andres, M. Phase recovery by using optical fiber dispersion. *Opt. Lett.* **2014**, *39*, 598–601. [CrossRef]
71. Cuadrado-Laborde, C.; Brotons-Gisbert, M.; Serafino, G.; Bogoni, A.; Pérez-Millán, P.; Andrés, M. Phase recovery by using optical fiber dispersion and pulse pre-stretching. *Appl. Phys. B* **2014**, *117*, 1173–1181. [CrossRef]
72. Karar, A.S. Iterative Algorithm for Electronic Dispersion Compensation in IM/DD Systems. *J. Light. Technol.* **2020**, *38*, 698–704. [CrossRef]
73. Goeger, G.; Prodaniuc, C.; Ye, Y.; Zhang, Q. Transmission of intensity modulation-direct detection signals far beyond the dispersion limit enabled by phase-retrieval. In Proceedings of the 2015 European Conference on Optical Communication (ECOC), Valencia, Spain, 27 September–1 October 2015; pp. 1–3. [CrossRef]
74. Wu, X.; Karar, A.S.; Zhong, K.; Lau, A.P.T.; Lu, C. Experimental demonstration of pre-electronic dispersion compensation in IM/DD systems using an iterative algorithm. *Opt. Express* **2021**, *29*, 24735–24749. [CrossRef]
75. Zou, D.; Li, F.; Wang, W.; Yin, M.; Sui, Q.; Li, Z. Modified Gerchberg-Saxton Algorithm Based Electrical Dispersion Pre-Compensation for Intensity-modulation and Direct-detection Systems. *J. Light. Technol.* **2022**, *40*, 2840–2849. [CrossRef]
76. Zou, D.; Wang, W.; Yin, M.; Sui, Q.; Li, Z.; Li, F. Performance Enhanced Gerchberg-Saxton Algorithm Based Electrical Dispersion Pre-compensation for Intensity-Modulation and Direct-Detection System. In Proceedings of the Asia Communications and Photonics Conference 2021, Shanghai, China, 24–27 October 2021; p. W1B.3.
77. Yin, M.; Zou, D.; Wang, W.; Li, F.; Li, Z. Transmission of a 56-Gbit/s PAM4 signal with low-resolution DAC and pre-equalization only over 80 km fiber in C-band IM/DD systems for optical interconnects. *Opt. Lett.* **2021**, *46*, 5615–5618. [CrossRef] [PubMed]
78. Hu, S.; Zhang, J.; Tang, J.; Jin, W.; Giddings, R.; Qiu, K. Data-Aided Iterative Algorithms for Linearizing IM/DD Optical Transmission Systems. *J. Light. Technol.* **2021**, *39*, 2864–2872. [CrossRef]
79. Hu, S.; Zhang, J.; Tang, J.; Jin, T.; Jin, W.; Liu, Q.; Zhong, Z.; Giddings, R.; Hong, Y.; Xu, B.; et al. Multi-constraint Gerchberg-Saxton iteration algorithms for linearizing IM/DD transmission systems. *Opt. Express* **2022**, *30*, 10019–10031. [CrossRef] [PubMed]
80. Jin, X.; Jin, W.; Zhong, Z.; Jiang, S.; Rajbhandari, S.; Hong, Y.; Philip Giddings, R.; Tang, J. Error-Controlled Iterative Algorithms for Digital Linearization of IMDD-Based Optical Fibre Transmission Systems. *J. Light. Technol.* **2022**, *40*, 6158–6167. [CrossRef]
81. Wu, X.; Karar, A.S.; Zhong, K.; Gürkan, Z.N.; Lau, A.P.T.; Lu, C. Gerchberg-Saxton Based FIR Filter for Electronic Dispersion Compensation in IM/DD Transmission Part II: Experimental Demonstration and Analysis. *J. Light. Technol.* **2023**, *41*, 1428–1435. [CrossRef]
82. Chen, H.; Huang, H.; Fontaine, N.K.; Ryf, R. Phase retrieval with fast convergence employing parallel alternative projections and phase reset for coherent communications. *Opt. Lett.* **2020**, *45*, 1188–1191. [CrossRef]
83. Chen, H.; Fontaine, N.K.; Gené, J.M.; Ryf, R.; Neilson, D.T.; Raybon, G. Full-field, carrier-less, polarization-diversity, direct detection receiver based on phase retrieval. In Proceedings of the 45th European Conference on Optical Communication (ECOC 2019), Dublin, Ireland, 22–26 September 2019; pp. 1–3. [CrossRef]
84. Xiang, M.; Zhou, P.; Ye, B.; Fu, S.; Xu, O.; Li, J.; Peng, D.; Wang, Y.; Qin, Y. Adaptive intensity transformation-based phase retrieval with high accuracy and fast convergence. *Opt. Lett.* **2021**, *46*, 3215–3218. [CrossRef]
85. Ji, H.; Sun, M.; Sun, C.; Shieh, W. carrier-assisted differential detection with a generalized transfer function. *Opt. Express* **2020**, *28*, 35946–35959. [CrossRef]
86. Zhu, Y.; Li, L.; Fu, Y.; Hu, W. Symmetric carrier-assisted differential detection receiver with low-complexity signal-signal beating interference mitigation. *Opt. Express* **2020**, *28*, 19008–19022. [CrossRef]
87. Che, D.; Sun, C.; Shieh, W. Optical Field Recovery in Stokes Space. *J. Light. Technol.* **2019**, *37*, 451–460. [CrossRef]
88. Chen, H.; Fontaine, N.K.; Essiambre, R.J.; Huang, H.; Mazur, M.; Ryf, R.; Neilson, D.T. Space-Time Diversity Phase Retrieval Receiver. In Proceedings of the 2021 Optical Fiber Communications Conference and Exhibition (OFC), San Francisco, CA, USA, 6–10 June 2021; pp. 1–3.